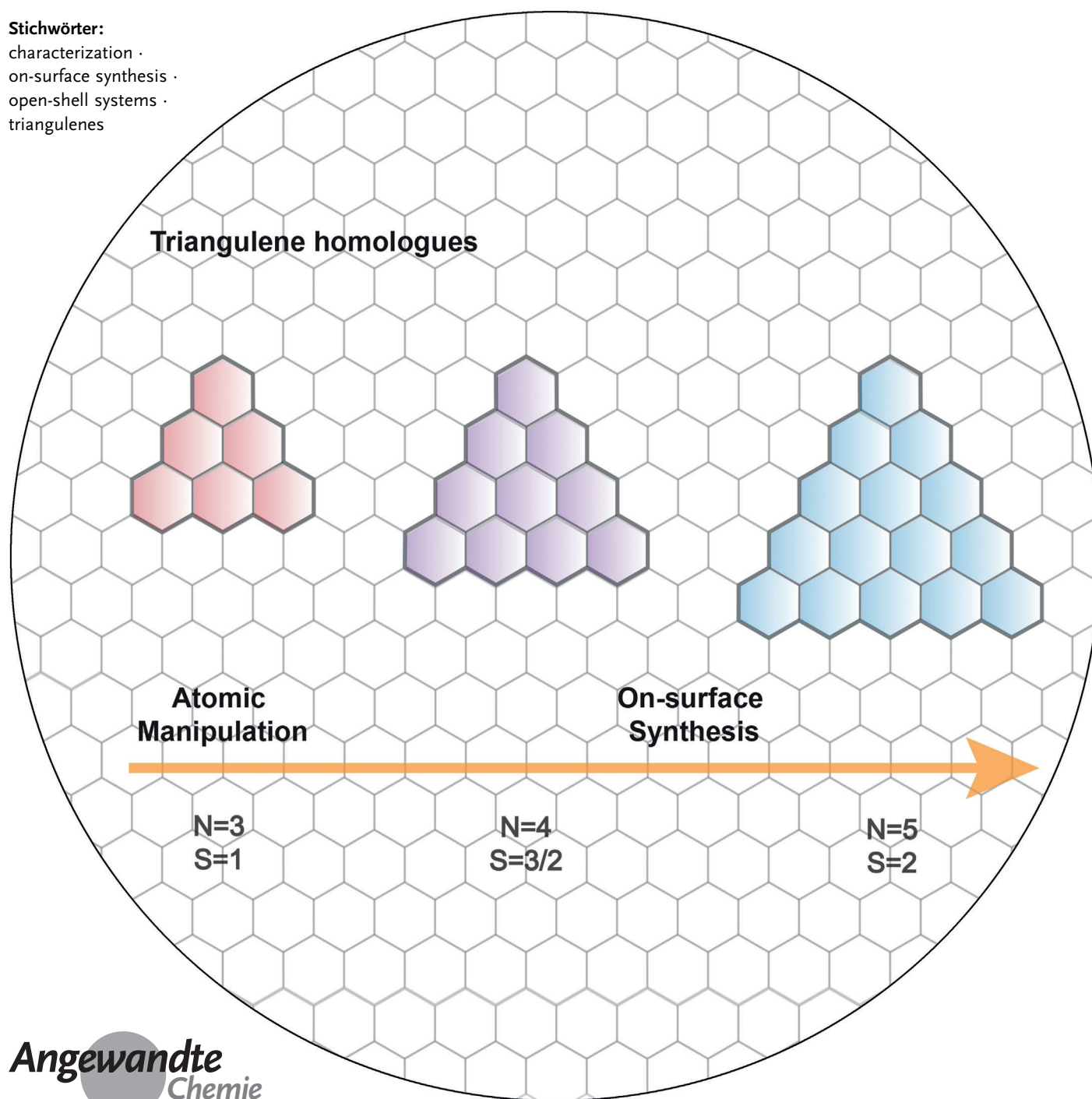


# Triangulenes: from Precursor Design to On-Surface Synthesis and Characterization

Jie Su, Mykola Telychko, Shaotang Song und Jiong Lu\*

**Stichwörter:**

characterization ·  
on-surface synthesis ·  
open-shell systems ·  
triangulenes



*Triangulene and its higher homologues are a class of zigzag-edged triangular graphene molecules (ZTGMs) with high-spin ground states. These open-shell molecules are predicted to host ferromagnetically coupled edge states with net spin values scaling with molecular size and are therefore considered promising candidates for future molecular spintronics applications. Unfortunately, the synthesis of unsubstituted [n]triangulenes and the direct observation of their edge states have been a long-standing challenge due to a high reactivity towards oxygen. However, recent advances in precursor design enabled the on-surface synthesis and characterization of unsubstituted [3]-, [4]-, and [5]triangulene. In this Minireview, we will highlight key aspects of this rapidly developing field, ranging from the principles of precursor design to synthetic strategies and characterization of a homologous series of triangulene molecules synthesized on-surface. We will also discuss challenges and future directions.*

## 1. Introduction

The extension of fused benzene rings in a triangular shape leads to a series of open-shell zigzag-edged triangular graphene molecules (ZTGMs) such as the monoradical phenalenyl ( $n=2$ ), the diradical [3]triangulene ( $n=3$ ), the  $\pi$ -extended triradical [4]triangulene ( $n=4$ ), the tetraradical [5]triangulene ( $n=5$ ), and the pentaradical [6]triangulene ( $n=6$ ), where  $n$  is the number of carbon atoms at each zigzag edge (Figure 1 a).<sup>[1–4]</sup> The unique triangular topology of these compounds combined with the zigzag edges makes it impossible to construct Kekulé resonance structures without unpaired electrons.<sup>[5]</sup> Therefore, these molecules are also known as non-Kekulé polynuclear benzenoid compounds with open-shell character. Triangulene and its higher homologues ( $n \geq 3$ ) are predicted to possess multiple unpaired  $\pi$ -electrons with net spins scaling linearly with  $n$ . Hence, these open-shell graphene-like molecules hold great promise as key components for utilization in next-generation molecular spintronics.<sup>[6]</sup> The total net spin of these compounds can be quantified based on the Ovchinnikov rule established by Lieb's theorem for bipartite lattices.<sup>[7,8]</sup> The rule describes the ground-state spin quantum number as  $S = \frac{(N_A - N_B)}{2}$ , where  $N_A$  and  $N_B$  denote the number of carbon atoms from the two interpenetrating triangular sublattices, respectively (marked in red and blue color in Figure 1 a). Because of the inherent sublattice imbalance, not all  $\pi$ -electrons can be paired to form  $\pi$ -bonds, leading to the formation of  $\pi$ -radicals. Additionally, the most stable ferromagnetic high-spin states of these ZTGMs have been theoretically described at different approximation levels, including tight-binding models and spin-polarized density functional theory (DFT) with many-body corrections.<sup>[5,9–13]</sup>


Due to unique electronic and magnetic properties, the triangulene series has fascinated scientists for many decades. However, the synthesis of unsubstituted triangulenes via

conventional wet-chemistry approaches has been deemed a formidable challenge due to their high chemical reactivity arising from the edge-localized  $\pi$ -radicals.<sup>[14,15]</sup> In this regard, the on-surface synthesis of these molecules under ultra-high vacuum (UHV) conditions provides a promising approach for the synthesis and characterization of unsubstituted ZTGMs. In contrast to the wet-chemistry approach, on-surface synthesis typically involves the use of catalytically active substrates for the catalytic transformation of well-designed molecular precursors into desired products at elevated temperatures.<sup>[16,17]</sup> Furthermore, the as-synthesized molecules can be directly characterized in detail using high-resolution imaging techniques such as scanning tunnelling microscopy (STM) and non-contact atomic force microscopy (ncAFM).<sup>[18–27]</sup>

The field of on-surface synthesis has advanced rapidly over the past decade, especially in the synthesis of atomically precise graphene nanoribbons (GNRs) and unsubstituted higher acenes.<sup>[28–32]</sup> Cai et al. reported a pioneering work on the bottom-up fabrication of GNRs on Au(111) in 2010.<sup>[33]</sup> Since then, a diversity of GNRs with different widths, edge configurations, and hetero-dopants have been synthesized on different substrates.<sup>[34–39]</sup> The common strategy for on-surface synthesis of GNRs involves the cyclodehydrogenation of designed precursor monomers or polymerized monomers via intramolecular or intermolecular aryl–aryl coupling, which occurs predominantly along the armchair direction rather than the zigzag direction.<sup>[36]</sup> Therefore, a majority of graphene nanostructures synthesized to date contains armchair edges.<sup>[40–44]</sup> It also remains a grand challenge to design appropriate molecular precursors for the synthesis of large homologues of ZTGMs with predicted large net spins. In this Minireview, we will highlight recent synthetic strategies towards the on-surface synthesis of a homologous series of [n]triangulenes. We will also discuss the electronic and magnetic properties of these high-spin molecules.

[\*] J. Su, M. Telychko, S. Song, J. Lu  
Department of Chemistry, National University of Singapore  
3 Science Drive 3, Singapore 117543 (Singapore)  
E-Mail: chmluj@nus.edu.sg

J. Su, M. Telychko, J. Lu  
Centre for Advanced 2D Materials (CA2DM)  
National University of Singapore  
6 Science Drive 2, Singapore 117546 (Singapore)

 The ORCID identification number(s) for the author(s) of this article can be found under:  
<https://doi.org/10.1002/anie.201913783>.

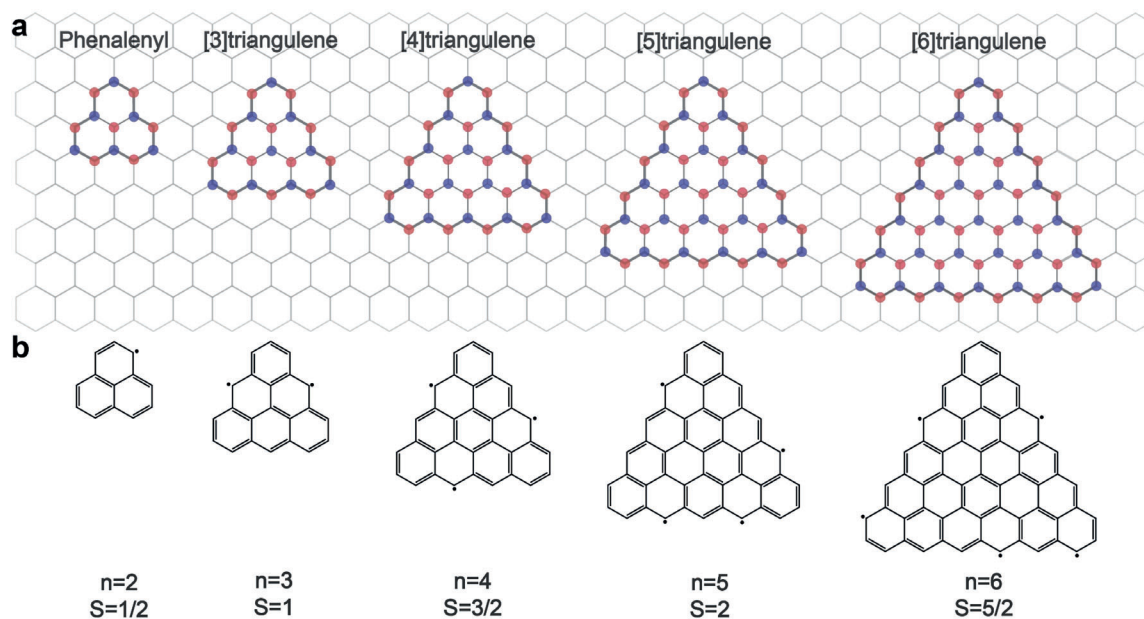
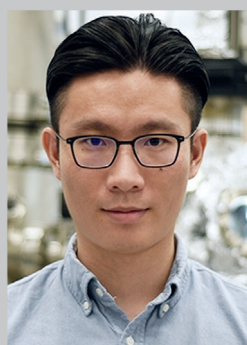


**Figure 1.** a) Illustration of open-shell ZTGMs with different numbers of zigzag carbon atom ( $n$ ) and predicted spin multiplicity ( $S$ ). The red and blue spots represent two interpenetrating triangular sublattices. b) The corresponding non-Kekulé structures with unpaired electrons of these ZTGMs. Please note that [6]triangulene has not been obtained experimentally.

## 2. Tip-Assisted Synthesis and Characterization of [3]Triangulene

In 2017, Pavliček and co-workers reported a seminal work on the synthesis of unsubstituted [3]triangulene by means of

atomic manipulation.<sup>[45]</sup> The STM tip was used to dehydrogenate molecular precursors consisting of a mixture of dihydrotriangulene isomers. The tip-assisted removal of a single hydrogen atom from the  $\text{CH}_2$  groups of two dihydrotriangulene isomers with higher resonance energy



Jie Su is a PhD candidate in the Department of Chemistry, Centre for Advanced 2D Materials, National University of Singapore (NUS). He received his M.Sc. from the National University of Singapore in 2014, after which he joined Prof. Jiong Lu's research group in 2015 as a PhD student. His current research topic focuses on the on-surface synthesis and characterization of graphene nanostructures using scanning tunneling microscopy and non-contact atomic force microscope.



Dr. Shaotang Song received his M.Sc. in 2014 from the Beijing Institute of Technology and obtained his PhD in 2017 under the supervision of Professor Hiroshi Sakaguchi at Kyoto University. He joined the groups of Hiromitsu Maeda at Ritsumeikan University in 2018 and, afterwards, Jiong Lu at the National University of Singapore for postdoctoral research. His current research focuses on the bottom-up on-surface synthesis and characterization of graphene nanostructures via a combination of organic synthesis and scanning tunneling microscopy.



Dr. Mykola Telychko received his M.Sc. in 2012 from the Department of Physics of Uzhgorod, National University of Ukraine. He obtained his PhD degree in 2016 under the supervision of Prof. Pavel Jelínek at the Institute of Physics, Academy of Science of Czech Republic. Afterwards, he joined the group of Prof. Jiong Lu at the Department of Chemistry, National University of Singapore as a postdoctoral researcher. His current research topics include studying novel 2D materials and bottom-up-synthesized graphene-like nanostructures with high-resolution scanning-probe-microscopy techniques.



Dr. Jiong Lu is currently an Assistant Professor at the Department of Chemistry, Centre for Advanced 2D Materials, National University of Singapore (NUS). He received his B.Sc. from Fudan University (China) in 2007 and his PhD degree from NUS in 2011. Afterwards, he worked as a postdoc in the Graphene Research Centre, NUS, and joined Mike Crommie's group at the Department of Physics, UC, Berkeley, for postdoctoral research. His current research interests include atomic-scale imaging and characterization of 2D materials and gate-tunable devices, as well as single-atom catalysis for energy-related applications.

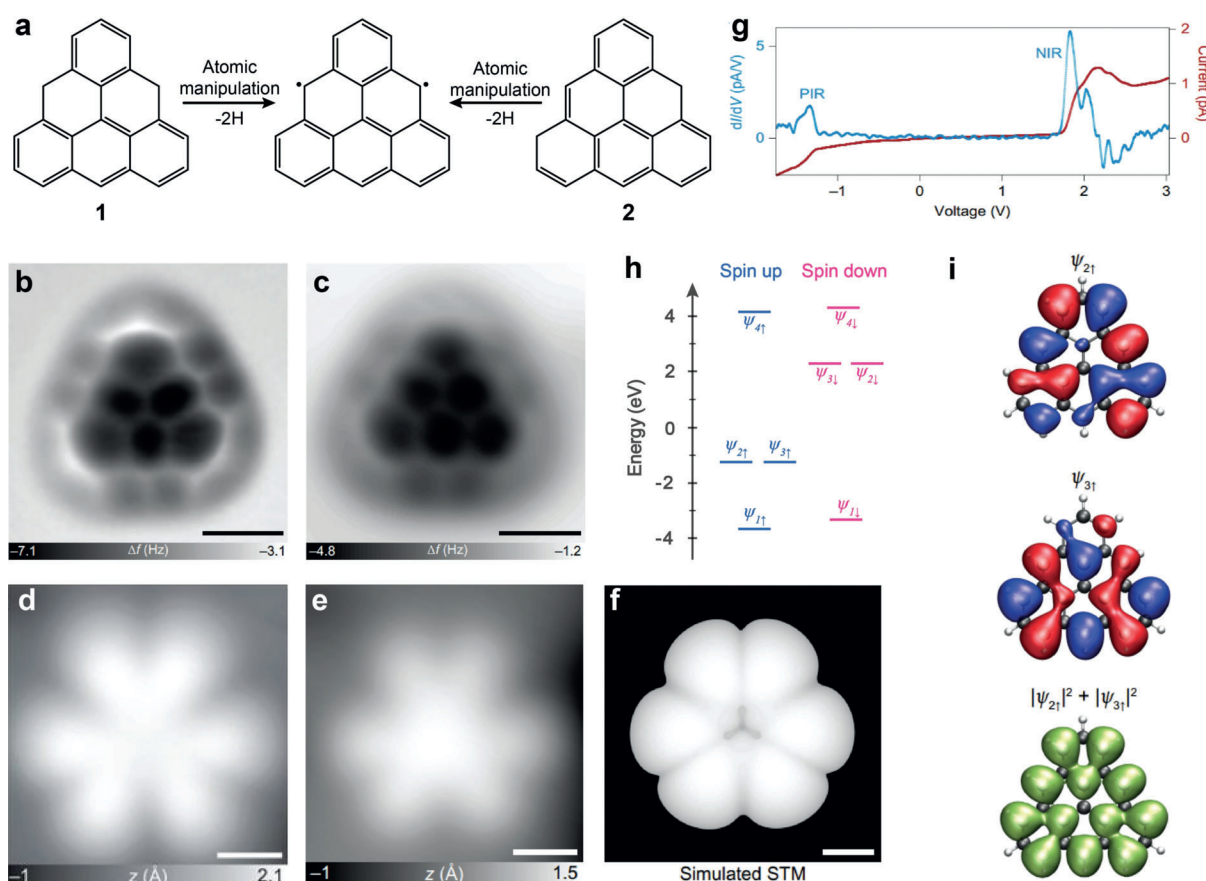


**Figure 2.** a) Generation of [3]triangulene from two precursor isomers (1 and 2) via tip-assisted manipulation. b), c) nAFM images of [3]triangulene synthesized on Cu(111) and a monolayer Xe island. d), e) STM images of [3]triangulene at the bias voltage of d) the negative-ion resonance (NIR) and e) the positive-ion resonance (PIR). f) Simulated STM image of degenerate orbitals  $\psi_{2\uparrow}$  and  $\psi_{3\uparrow}$  with an s-orbital-like tip. g) Experimental  $dI/dV$  spectra recorded over a [3]triangulene molecule on a Xe island. h) Energy diagram derived from the spin-polarized DFT calculation of [3]triangulene. i) Plots of the DFT-calculated wave functions of  $\psi_{2\uparrow}$  and  $\psi_{3\uparrow}$  and the sum of their probability densities ( $|\psi_{2\uparrow}|^2 + |\psi_{3\uparrow}|^2$ ). Adapted with permission from Ref. [40]. Copyright 2017 Springer Nature.

was performed to generate [3]triangulene molecules on different surfaces (Figure 2a). The tip-assisted manipulation process involves the following critical steps: i) position the tip over the molecule; ii) open the feedback loop iii) retract the tip by a few Å; iv) increase bias voltage to the range from 3.5 to 4.1 V for several seconds. In general, this process needs to be applied twice to an individual dihydrotriangulene to make a single [3]triangulene. It should be noted that the manipulation process can be conducted over molecular precursors adsorbed on different substrates including Cu(111), bilayer NaCl, and monolayer Xe on Cu(111). [3]Triangulene synthesized on Cu(111) and Xe/Cu(111) surfaces shows a high adsorption stability, while the molecule undergoes frequent rotation on the NaCl surface, arising from the symmetry mismatch between the molecule and the square lattice of (100)-oriented NaCl surfaces. nAFM imaging of [3]triangulene adsorbed on both Cu(111) and Xe/Cu(111) substrates confirmed its  $C_3$  symmetry with six fused benzene rings (Figure 2b,c). It is worth noting that the brighter contrast of the zigzag carbon atoms in the nAFM image acquired of [3]triangulene on Cu(111) suggests that the carbon atoms at the zigzag edge are slightly bent away from the surface. This observation implies a  $\pi$ -radical character of [3]triangulene on

Cu(111) distinct from the reported  $\sigma$  radicals that tend to form strong covalent bonds with the Cu substrate.<sup>[46–48]</sup>

STM orbital imaging and scanning tunneling spectroscopy (STS) were used to probe the peculiar electronic structures of [3]triangulene adsorbed on Xe/Cu(111). The differential conductance ( $dI/dV$ ) as a function of voltage acquired above the center of a [3]triangulene molecule reveals two prominent features centered at  $V = -1.4$  V and  $V = 1.85$  V. The feature below (above) the Fermi level corresponds to the positive-ion resonance (negative-ion resonance), leading to an energy gap of 3.25 eV (Figure 2g). Additionally, STM images collected at sample biases corresponding to negative-ion resonance (1.85 V) and positive-ion resonance ( $-1.4$  V) exhibit the same nodal pattern along the zigzag edges (Figure 2d,e).

Spin-polarized DFT calculations of an isolated [3]triangulene molecule predict that the triplet state (ferromagnetic) is energetically more favorable than the closed-shell (non-magnetic) and open-shell singlet states (antiferromagnetic) by 0.35 and 0.16 eV, respectively. It is also found that [3]triangulene adsorbed on Xe/Cu(111) favors the triplet state by 0.33 eV over the closed-shell singlet state. The closed-shell singlet state, featuring degenerate frontier orbitals, would result in a cationic state due to charge transfer between

the adsorbed molecule and the substrate. This is in contrast to the neutral-charge state of [3]triangulene on Xe films and NaCl, as evidenced by the absence of scattering of the interface electrons in the STM image. Therefore, these observations also help to rule out the non-magnetic closed-shell state of [3]triangulene.

Since STS measurements probe excited states of molecular adsorbates, the authors also performed spin-polarized DFT calculations including many-body corrections in the  $G_0W_0$  approximation to understand the features observed in the experimental  $dI/dV$  spectra. The calculated energy level of the triplet ground state of [3]triangulene is shown in Figure 2h. The frontier molecular orbitals are two pairs of spin-polarized degenerate orbitals ( $\psi_2$  and  $\psi_3$ ). The energy gap between the pair of occupied states (spin-up) and the pair of empty states (spin-down) is predicted to be 3.78 eV. The difference between the calculated gap and the experimentally observed gap (3.25 eV) can be attributed to electronic screening of the substrate. Additionally, the simulated STM image of a degenerate pair of spin-up orbitals ( $\psi_{2\uparrow}$  and  $\psi_{3\uparrow}$ ) probed with an s-orbital-like tip wave function closely resembles the experimental orbital images, which suggests that the superposition of  $\psi_{2\uparrow}$  and  $\psi_{3\uparrow}$  is probed in STM imaging. Both experimental and theoretical results confirm the successful synthesis of [3]triangulene on Xe/Cu(111) with a triplet ground state. This work demonstrates a completely new route for the synthesis of the smallest unsubstituted triangulene molecules. Moreover, the tip-assisted synthesis of [3]triangulene can be performed on insulating surfaces, where the electronic structure of the molecule is decoupled from the substrate. Therefore, this opens up new possibilities for the further exploration of spin excitations at the single-molecule level. However, since only one target molecule can be manipulated at a time, this method is only useful for particular applications and may not be suitable for other technological applications due to a lack of scalability.

### 3. On-Surface Synthesis and Characterization of Higher Triangulene Homologues

To synthesize the ZTGs (for example, [4]- and [5]triangulene) in a large quantity, a rational design of new organic precursors is required. Inspired by the synthesis of zigzag-edged graphene nanoribbons (ZGNRs), methyl groups can be introduced at the appropriate positions of the molecular precursors to form zigzag edges. At elevated temperatures, the methyl group and the neighboring benzene ring can undergo cyclodehydrogenation to form a new benzene ring with zigzag edges. A similar strategy can be adapted to design molecular precursors for the scalable synthesis of large triangulene homologues. We will highlight two recent works on the atomically precise synthesis of  $\pi$ -extended triangulenes on different metal substrates. Lu and co-workers have demonstrated the successful synthesis of [5]triangulene on both Au(111) and Cu(111) substrates. Ruffieux et al. also reported the synthesis of [4]triangulene on Au(111).<sup>[49,50]</sup>

#### 3.1. Synthesis and Characterization of [4]Triangulene

[4]triangulene, which consists of ten benzene rings fused in a triangular shape, is predicted to have a net spin of  $S = 3/2$  (Figure 3a). The precursor contains three methyl substituents attached to a benzo[*c*]naphtho[2,1-*p*]chrysene core (Figure 4a). These methyl groups can undergo surface-catalyzed oxidative ring-closure reactions at high temperatures, leading to the formation of [4]triangulene. Au(111) with a submonolayer coverage of molecular precursors was annealed up to 600 K to promote the cyclodehydrogenation reactions. Bond-resolved STM imaging performed in the Pauli-repulsion regime using a CO-functionalized tip reveals the structure of the threefold-symmetric products resembling the molecular backbone, which confirms the successful formation of [4]triangulene (Figure 3c). The planar adsorption of the products on Au(111) also suggests an absence of any chemical bonding to the surface, presumably due to the  $\pi$ -radical character of [4]triangulene.

The electronic structure of [4]triangulene is described using the nearest-neighbor tight-binding model (TB), including electron-correlation effects. Inclusion of on-site Coulomb repulsion ( $U$ ) within the mean-field Hubbard (MFH) mode induces spin polarization, resulting in the formation of three nearly degenerate singly occupied molecular orbitals (SOMOs; Figure 3f). The ferromagnetic spin alignment of the electrons populating the SOMOs gives rise to the open-shell quartet ground state, lower in energy by 236 meV compared to the open-shell doublet state. Furthermore, the calculated spin-polarized wave functions of the SOMOs (Figure 3j) exhibit an edge-localized character with maximum amplitude on one sublattice. The  $dI/dV$  spectrum acquired over the corner of the molecule reveals two broad features peaking around  $-0.40$  V and  $+1.15$  V, corresponding to the positive- and negative-ion resonances, respectively. Moreover, the simulated local-density-of-states (LDOS) maps of the SOMOs and the corresponding unoccupied orbitals (SUMOs; Figure 3h,i) reproduce the features captured in the spatial  $dI/dV$  maps taken at  $-0.40$  V and  $+1.15$  V, respectively (Figure 3d,e). Therefore, STM and STS measurements combined with theoretical calculations confirm the successful synthesis of [4]triangulene on Au(111) with an open-shell quartet ground state.<sup>[49]</sup>

#### 3.2. Synthesis and Characterization of [5]Triangulene

We reported a bottom-up on-surface synthesis of [5]triangulene, which contains 15 fused benzene rings, making it the largest unsubstituted triangulene homologue synthesized so far.<sup>[50]</sup> To achieve this goal, we designed a unique precursor containing a central triangular core formed by six hexagonal rings and three 2,6-dimethylphenyl substituents attached at the *meso*-positions of the core. This precursor can be obtained via multiple synthetic steps starting from 9-bromo-10-(2,6-dimethylphenyl)-anthracene (Figure 4a). It is expected that two hydrogen atoms connected to the two  $sp^3$ -carbons of the core undergo the surface-catalyzed dehydrogenation first due to a higher stability of the as-formed triphenylmethyl radicals

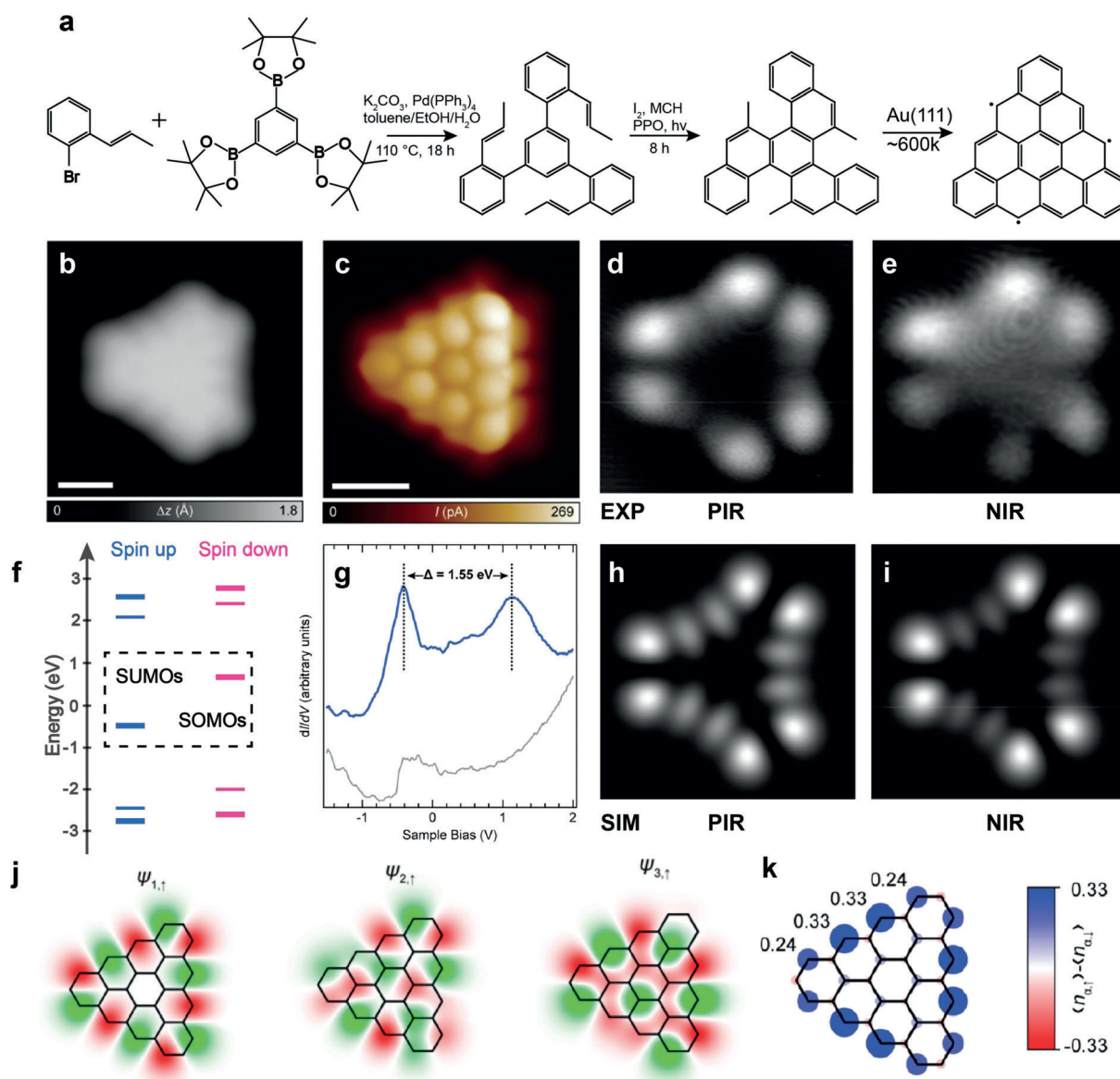


**Figure 3.** a) Synthetic route for [4]triangulene. b) STM image of an isolated [4]triangulene molecule on Au(111). c) Ultra-high-resolution STM image of [4]triangulene acquired with a CO-functionalized tip. d), e) Constant-current  $dI/dV$  maps of [4]triangulene at the bias of the PIR (f) and the NIR (g). f) Calculated energy diagram of a [4]triangulene using MFH model with spin-polarization. g) Experimental  $dI/dV$  spectra of a [4]triangulene on Au(111). h), i) Simulated  $dI/dV$  maps corresponding to (d) and (e). j) Calculated wave functions of the SOMOs of [4]triangulene. k) Computed spin-density distribution of [4]triangulene. Blue/red isosurfaces denote spin up/down density. Numbers denote spin-density values. Adapted with permission from Ref. [44]. Copyright 2019 American Chemical Society.

compared to benzylic radicals. Subsequently, the dehydrogenation of the six methyl groups occurs to generate benzylic radicals, which can attack the neighboring carbon atoms of the triangular core. In the last step, an aromaticity-driven ring-closure reaction leads to the formation of [5]triangulene.

We then deposited the molecular precursor onto both Cu(111) and Au(111) surfaces via thermal sublimation under UHV conditions. Annealing the precursor-decorated Cu(111) substrate at  $\approx 500$  K resulted in the formation of flat triangle-shaped molecules that matched to the expected [5]triangulene (Figure 4a). In contrast to Cu(111), the synthesis of [5]triangulene on the relatively inert Au(111) substrate had to be carried out at a higher temperature ( $\approx 600$  K) and gave

a much lower yield ( $\approx 5\%$ ) of the product. Magnified STM images show that individual molecules adopt a triangular and planar configuration after thermal annealing (Figure 4b,c). Additionally, the edges of the as-obtained molecules on both substrates exhibit the characteristic nodal features, resembling the zigzag termini or zigzag edges of GNRs.<sup>[51]</sup> As shown in Figure 4d,e, ncAFM images performed in constant-height mode with a CO-functionalized tip clearly resolve 15 fused benzene rings with a zigzag-edged topology for individual triangle-shaped products. Moreover, the absence of a bonding signature of [5]triangulene to the supporting substrates can also be ascribed to the  $\pi$ -radical nature of its zigzag edges. Hence, the observed molecular morphology directly confirms

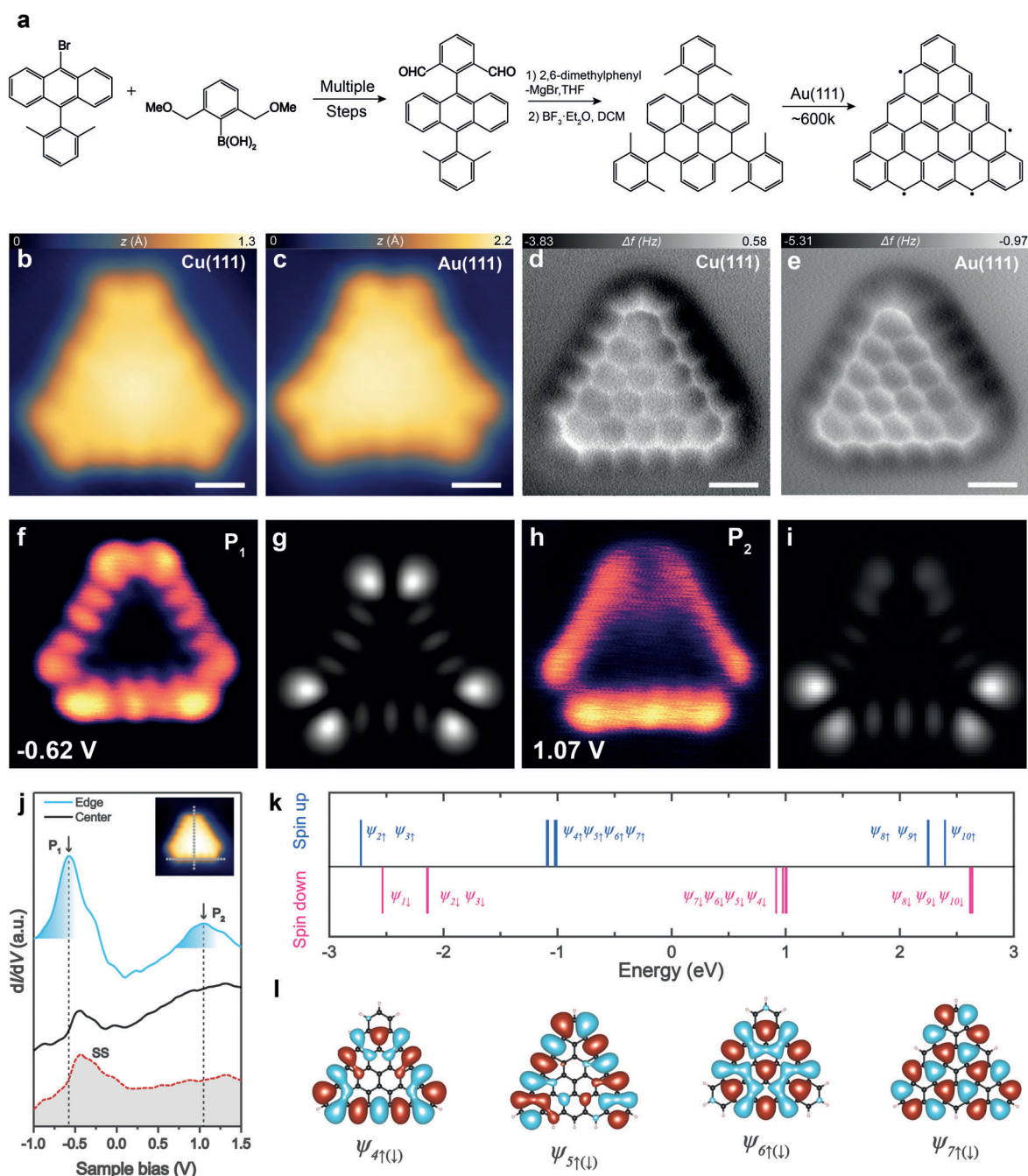


**Figure 4.** a) Synthetic route for [5]triangulene. b), c) STM images of [5]triangulene synthesized on Cu(111) and Au(111). d), e) nAFM images of a single [5]triangulene on d) Cu(111) and e) Au(111). f), h)  $dI/dV$  maps of [5]triangulene on Au(111) acquired at the bias voltage of f)  $P_1$  and h)  $P_2$ . g), i) Simulated  $dI/dV$  maps at the energy of g)  $P_1$  and i)  $P_2$ . j)  $dI/dV$  spectra of a [5]triangulene molecule on Au(111). k) Calculated spin-polarized molecular orbital energies of an isolated [5]triangulene molecule. l) DFT-calculated wave functions of four degenerate spin-polarized orbitals. Adapted with permission from Ref. [45]. Copyright 2019 American Association for the Advancements of Science.

the successful synthesis of [5]triangulene on both metal substrates.

To unveil the electronic structure of [5]triangulene, STS was performed over a single [5]triangulene molecule synthesized on the weakly interacting Au(111) substrate using a metallic tip. The  $dI/dV$  spectrum acquired at the molecular edge (blue curve) shows two prominent peaks at  $V_S = -0.62 \pm 0.04$  V ( $P_1$ ) and  $V_S = 1.07 \pm 0.04$  V ( $P_2$ ). In contrast, the  $dI/dV$  spectrum acquired over the center of molecule does not

exhibit these two features (black curve) (Figure 4j). These observations suggest that both  $P_1$  and  $P_2$  states are presumably associated with the edge states of [5]triangulene. Spin-polarized DFT calculations show that the quintuple ground state of Au-supported [5]triangulene is lower in energy by 0.13 eV, 0.27 eV, and 0.38 eV than its triplet, open-shell singlet, and closed-shell singlet states, respectively. Figure 4k depicts the calculated spin-polarized energy levels of a free [5]triangulene in the ferromagnetic quintuple state. The

frontier molecular orbitals are four pairs of orbitals ( $\psi_{4\uparrow(\downarrow)}$ ,  $\psi_{5\uparrow(\downarrow)}$ ,  $\psi_{6\uparrow(\downarrow)}$ ,  $\psi_{7\uparrow(\downarrow)}$ ) in Figure 4k) with the corresponding wave functions shown in Figure 4l. Each (unoccupied) spin-down orbital is accompanied by a counterpart (occupied) spin-up orbital arising from the spin-polarized orbital splitting. From the energy-level alignment, it is expected that the neutral state of [5]triangulene should produce frontier-orbital-associated resonances below and above the Fermi level. As illustrated in Figure 4k, the nearly-degenerate spin-up states ( $\psi_{4\uparrow}$ ,  $\psi_{5\uparrow}$ ,  $\psi_{6\uparrow}$ ,  $\psi_{7\uparrow}$ ) and spin-down states ( $\psi_{4\downarrow}$ ,  $\psi_{5\downarrow}$ ,  $\psi_{6\downarrow}$ ,  $\psi_{7\downarrow}$ ) are energetically close to states  $P_1(-0.62\text{ V})$  and  $P_2(1.07\text{ V})$ , respectively.

The differential conductance map collected at the energy of  $P_1$  state ( $-0.62\text{ eV}$ ) reveals five bright lobes located at the edge of [5]triangulene, represented by a characteristic nodal pattern (Figure 4f). The  $dI/dV$  map acquired at  $1.07\text{ V}$  (Figure 4h) shows that the  $P_2$  state also exhibits an edge-localized pattern, resembling that of the  $P_1$  state, but with a slightly blurred nodal structure. The calculated  $dI/dV$  images of the four nearly degenerate orbitals ( $\psi_{4\uparrow}$ ,  $\psi_{5\uparrow}$ ,  $\psi_{6\uparrow}$ ,  $\psi_{7\uparrow}$ ) using an s-orbital-like tip reveal three characteristic lobes located in the middle of the edges with a pair of brighter lobes at the apexes of the triangle. Such an edge-localized nodal pattern shows a good agreement with our experimental  $dI/dV$  map recorded at the energy of  $P_1$ . The slightly asymmetric contrast of the  $dI/dV$  maps in Figure 4h,i could arise from the different degrees of degeneracy of the spin-up and spin-down edge states, as predicted in the theoretical results (Figure 4k). This means that the weight of certain orbitals is lower because of different degrees of degeneracy of these frontier orbitals, giving rise to a slightly asymmetric contrast in the  $dI/dV$  map acquired at the individual energies. We also calculated the quasiparticle energies of a free [5]triangulene within the  $GW$  approximation of many-body perturbation theory. The quasiparticle gap of a free [5]triangulene is predicted to be  $2.81\text{ eV}$  based on the  $GW$  calculations. A direct comparison between the experimentally determined gap and the  $GW$ -predicted value yields a gap decrease of around  $1\text{ eV}$ , which can be attributed to the screening of the metallic substrate, consistent with previous studies of GNRs and other molecular systems with comparable size. All the observations discussed above point towards a magnetic ground state of [5]triangulene on Au(111), which is further supported by DFT calculations.<sup>[50]</sup>

#### 4. Conclusion and Outlook

The successful synthesis of the triangulene series enables their unique structures and peculiar properties to be explored at the single-molecule level. High-resolution molecular-imaging techniques can unambiguously resolve the planar and threefold-symmetric molecular skeleton of these ZTGMs, whereas STS measurements reveal spin-polarized edge states.<sup>[52–54]</sup> A comparison between electronic structures probed experimentally and spin-polarized DFT calculations implies that triangulene and its higher homologues synthesized on weakly interacting substrates retain their open-shell magnetic ground states. To better access the size-dependent

electronic and magnetic properties of triangulene molecules, it is suggested to synthesize them on insulating substrates including NaCl, metal oxide thin films, and hexagonal boron nitride monolayers grown on metal substrates.<sup>[45,55,56]</sup>

It will be of great interest to perform spin-polarized STM/STS measurements to characterize the ferromagnetic states of ZTGMs and to explore how these molecules couple with each other or interact with magnetic atoms. Creating the larger homologues of triangulene is predicted to not only increase their net spin but also the total number of excited spin states (Figure 1). Therefore, it is alluring to probe multiple spin excitations within a large-size open-shell ZTGM on insulating substrates via a combination of spin-polarized STM and electron spin resonance (ESR), which can uncover the fascinating magnetic properties of triangulene compounds for spin detection.<sup>[57,58]</sup> Moreover, polymerizing the triangulene unit into two-dimensional high-spin networks is of both fundamental and technological importance (Figure 5a). This also calls for the design of smart organic precursors from chemists.<sup>[3,59]</sup>

Apart from the tuning of the size of ZTGMs, the electronic and magnetic properties of ZTGMs can be further modified via doping through heteroatom substitution (for example, N or B).<sup>[60]</sup> It has been predicted that the total net spin of ZTGMs and the chemical stability of different spin states can be altered via B- and N-doping of these compounds.<sup>[61,62]</sup> This can be realized by introducing the heteroatoms into the molecular precursor. Furthermore, the ability to fabricate ZTGM heterojunctions also offers another promising approach to achieve the desired properties and functionalities of these hybrid systems. For example, Wang and co-workers predicted that a ZTGM segment fused with the ZGNR (Figure 5b) could serve as the key component for a spin filter.<sup>[63]</sup> The novel spin alignment and exotic interface states may arise at the heterojunctions of these hybrid structures. It is expected that the fabrication of such ZTGM junctions can be realized via on-surface coupling reactions between different building blocks deposited on the same surface.<sup>[17]</sup> Therefore, we expect that a variety of triangulene homologues and their heterostructures with novel properties can be fabricated via on-surface synthesis in the near future.

In addition to the synthesis of ZTGMs with specific spin states, a high level of spin control via the electric field is critical for unlocking their potential for future spintronic applications (Figure 5c,d).<sup>[64,65]</sup> For example, it has been predicted that the full spin polarization of charge-neutral ZTGMs can be quenched via either applying an electric field or adding extra electrons into these strongly correlated electronic systems (Figure 5e).<sup>[65–67]</sup> Recent experimental progresses have demonstrated the capability to control the charge state of a single molecule integrated with a back-gated graphene device.<sup>[68,69]</sup> We envision that such a field-controlled spin switch can be realized by synthesizing these ZTGMs on a back-gated device using tip-assisted manipulation. A field-controlled reversible spin switch at the single-molecule level potentially allows for the fabrication of single-molecule spintronics and ultra-high-capacity data-storage devices.



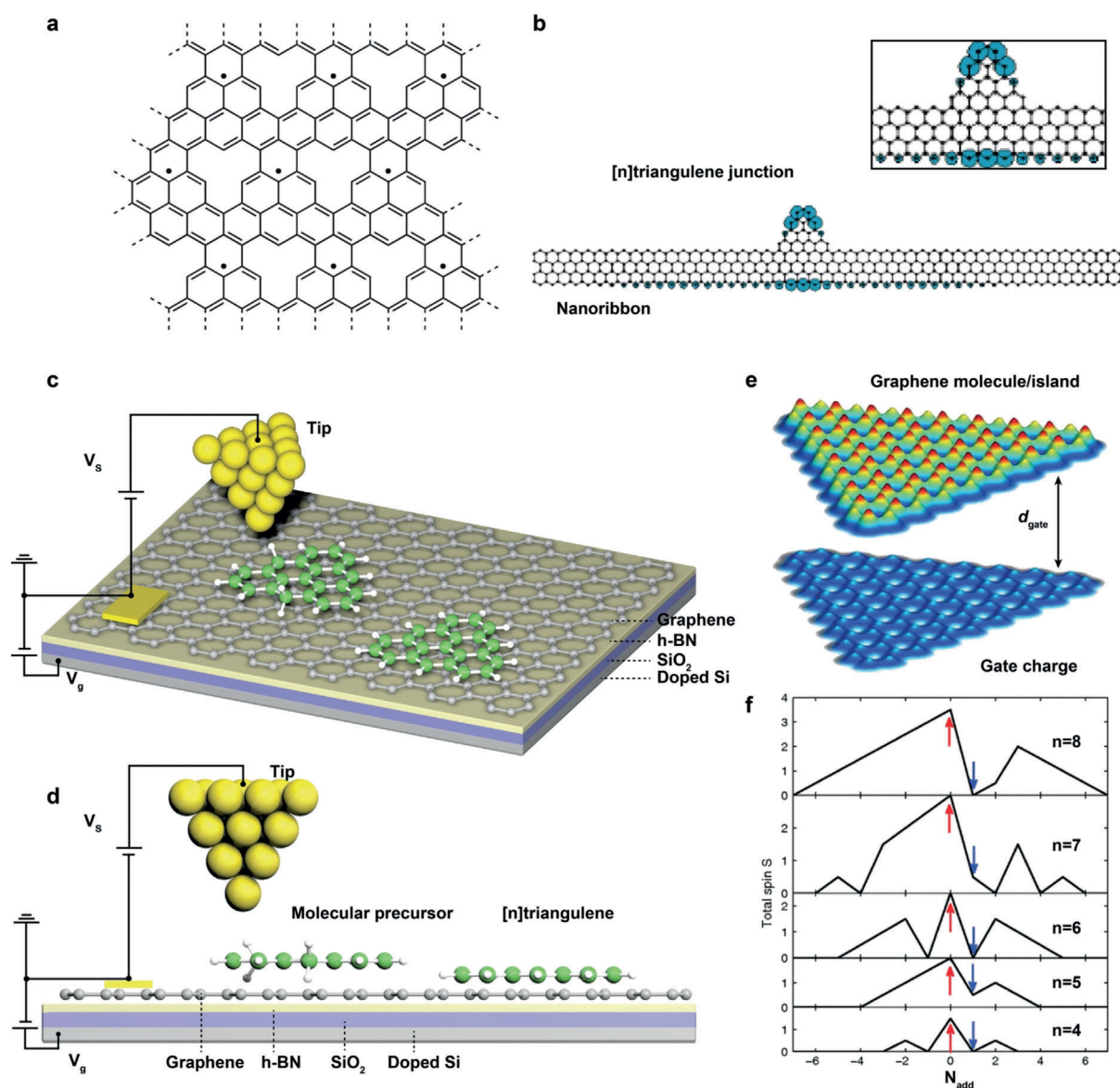


**Figure 5.** a) 2D magnetic triangulene network consisting of a high-spin polymeric neutral  $\pi$ -radical system. b) Calculated net spin density distribution of a triangulene molecule attached to a zigzag GNR. (Inset: magnified image of the triangulene junction with the calculated net spin density, which is projected from the nonbonding states obtained by the tight-binding approximation of the finite GNR system). c) Illustration of the synthesis of a  $[n]$ triangulene by tip manipulation on a back-gated graphene device. d) Side view of (c). e) Calculated electronic density in a  $[8]$ triangulene molecule of 97 carbon atoms, where 7 electrons from the degenerate orbitals are moved to the metallic gate at a distance of  $d_{\text{gate}}$ . f) Spin phase diagram for  $[n]$ triangulene molecules with different sizes (characterized by the number of zigzag-edged carbon atoms  $n$ ) as a function of the filling of the zero-energy states  $N_{\text{add}}$ , calculated by the tight-binding Hartree–Fock configuration-interaction method. The charge-neutral case corresponds to  $N_{\text{add}}=0$ , in which case the total spin of the zero-energy electrons is always maximized ( $S=n/2$ , indicated by red arrows). Adding one extra electron to the ZTGM corresponds to the case of  $N_{\text{add}}=1$ , where the total spin of the molecule is lowered to the minimum possible value, as indicated by blue arrows. a) Adapted with permission from Ref. [3]. Copyright 2011 Springer Nature. b) Adapted with permission from Ref. [61]. Copyright 2008 American Chemical Society. e), f) Adapted with permission from Ref. [65]. Copyright 2009 American Physical Society.

### Acknowledgements

J.L. acknowledges the support from MOE grants (MOE2017-T2-1-056 and R-143-000-A75-114).

### Conflict of interest

The authors declare no conflict of interest.

- [1] E. Clar, D. G. Stewart, *J. Am. Chem. Soc.* **1953**, *75*, 2667–2672.
- [2] M. Melle-Franco, *Nat. Nanotechnol.* **2017**, *12*, 292–293.
- [3] Y. Morita, S. Suzuki, K. Sato, T. Takui, *Nat. Chem.* **2011**, *3*, 197–204.
- [4] M. Ezawa, *Phys. Rev. B* **2007**, *76*, 245415–245416.
- [5] S. Fujii, T. Enoki, *Acc. Chem. Res.* **2013**, *46*, 2202–2210.
- [6] W. Han, R. K. Kawakami, M. Gmitra, J. Fabian, *Nat. Nanotechnol.* **2014**, *9*, 794–807.
- [7] A. A. Ovchinnikov, *Theor. Chim. Acta* **1978**, *47*, 297–304.
- [8] E. Lieb, *Phys. Rev. Lett.* **1989**, *62*, 1201–1204.
- [9] A. H. Castro Neto, F. Guinea, N. M. R. Peres, K. S. Novoselov, A. K. Geim, *Rev. Mod. Phys.* **2009**, *81*, 109–162.
- [10] M. Zarenia, A. Chaves, G. A. Farias, F. M. Peeters, *Phys. Rev. B* **2011**, *84*, 245403–245412.
- [11] P. Potasz, A. D. Güçlü, P. Hawrylak, *Phys. Rev. B* **2010**, *81*, 033403.
- [12] W. L. Wang, O. V. Yazyev, S. Meng, E. Kaxiras, *Phys. Rev. Lett.* **2009**, *102*, 195–194.
- [13] J. Fernández-Rossier, J. J. Palacios, *Phys. Rev. Lett.* **2007**, *99*, 177204.
- [14] G. Allinson, R. J. Bushby, J. L. Paillaud, D. Oduwole, K. Sales, *J. Am. Chem. Soc.* **1993**, *115*, 2062–2064.
- [15] G. Allinson, R. J. Bushby, M. V. Jesudason, J. L. Paillaud, N. Taylor, *J. Chem. Soc. Perkin Trans. 2* **1997**, 147–156.
- [16] A. Gourdon, *Angew. Chem. Int. Ed.* **2008**, *47*, 6950–6953; *Angew. Chem.* **2008**, *120*, 7056–7059.
- [17] S. Clair, D. G. de Oteyza, *Chem. Rev.* **2019**, *119*, 4717–4776.
- [18] F. J. Giessibl, *Rev. Mod. Phys.* **2003**, *75*, 949–983.
- [19] L. Gross, F. Mohn, N. Moll, P. Liljeroth, G. Meyer, *Science* **2009**, *325*, 1110–1114.
- [20] L. Gross, N. Moll, F. Mohn, A. Curioni, G. Meyer, F. Hanke, M. Persson, *Phys. Rev. Lett.* **2011**, *107*, 086101.
- [21] D. G. de Oteyza, P. Gorman, Y.-C. Chen, S. Wickenburg, A. Riss, D. J. Mowbray, G. Etkin, Z. Pedramrazi, H.-Z. Tsai, A. Rubio, et al., *Science* **2013**, *340*, 1434–1437.
- [22] L. Gross, F. Mohn, N. Moll, G. Meyer, R. Ebel, W. M. Abdel-Mageed, M. Jaspars, *Nat. Chem.* **2010**, *2*, 821–825.
- [23] A. Riss, A. P. Paz, S. Wickenburg, H.-Z. Tsai, D. G. de Oteyza, A. J. Bradley, M. M. Ugeda, P. Gorman, H. S. Jung, M. F. Crommie, A. Rubio, F. R. Fischer, *Nat. Chem.* **2016**, *8*, 678–683.
- [24] L. Gross, *Nat. Chem.* **2011**, *3*, 273–278.
- [25] N. Pavliček, L. Gross, *Nat. Rev. Chem.* **2017**, *1*, 0005.
- [26] F. J. Giessibl, *Rev. Sci. Instrum.* **2019**, *90*, 011101.
- [27] M. Telychko, J. Su, A. Gallardo, Y. Gu, J. I. Mendieta-Moreno, D. Qi, A. Tadich, S. Song, P. Lyu, Z. Qiu, et al., *Angew. Chem. Int. Ed.* **2019**, *58*, 18591–18597; *Angew. Chem.* **2019**, *131*, 18764–18770.
- [28] J. Krüger, F. García, F. Eisenhut, D. Skidin, J. M. Alonso, E. Guitián, D. Pérez, G. Cuniberti, F. Moresco, D. Peña, *Angew. Chem. Int. Ed.* **2017**, *56*, 11945–11948; *Angew. Chem.* **2017**, *129*, 12107–12110.
- [29] J. I. Urgel, H. Hayashi, M. Di Giovannantonio, C. A. Pignedoli, S. Mishra, O. Deniz, M. Yamashita, T. Dienel, P. Ruffieux, H. Yamada, et al., *J. Am. Chem. Soc.* **2017**, *139*, 11658–11661.
- [30] M. Zugermeier, M. Gruber, M. Schmid, B. P. Klein, L. Ruppenthal, P. Müller, R. Einholz, W. Hieringer, R. Berndt, H. F. Bettinger, et al., *Nanoscale* **2017**, *9*, 12461–12469.
- [31] R. Zuzak, R. Dorel, M. Krawiec, B. Such, M. Kolmer, M. Szymonski, A. M. Echavarren, S. Godlewski, *ACS Nano* **2017**, *11*, 9321–9329.
- [32] R. Zuzak, R. Dorel, M. Kolmer, M. Szymonski, S. Godlewski, A. M. Echavarren, *Angew. Chem. Int. Ed.* **2018**, *57*, 10500–10505; *Angew. Chem.* **2018**, *130*, 10660–10665.
- [33] J. Cai, P. Ruffieux, R. Jaafar, M. Bieri, T. Braun, S. Blankenburg, M. Muoth, A. P. Seitsonen, M. Saleh, X. Feng, et al., *Nature* **2010**, *466*, 470–473.
- [34] A. Kimouche, M. M. Ervasti, R. Drost, S. Halonen, A. Harju, P. M. Joensuu, J. Sainio, P. Liljeroth, *Nat. Commun.* **2015**, *6*, 10177.
- [35] L. Talirz, H. Söde, T. Dumsloff, S. Wang, J. R. Sanchez-Valencia, J. Liu, P. Shinde, C. A. Pignedoli, L. Liang, V. Meunier, et al., *ACS Nano* **2017**, *11*, 1380–1388.
- [36] P. Ruffieux, S. Wang, B. Yang, C. Sánchez-Sánchez, J. Liu, T. Dienel, L. Talirz, P. Shinde, C. A. Pignedoli, D. Passerone, et al., *Nature* **2016**, *531*, 489–492.
- [37] J. Cai, C. A. Pignedoli, L. Talirz, P. Ruffieux, H. Söde, L. Liang, V. Meunier, R. Berger, R. Li, X. Feng, et al., *Nat. Nanotechnol.* **2014**, *9*, 896–900.
- [38] Y.-C. Chen, T. Cao, C. Chen, Z. Pedramrazi, D. Haberler, D. G. de Oteyza, F. R. Fischer, S. G. Louie, M. F. Crommie, *Nat. Nanotechnol.* **2015**, *10*, 156–160.
- [39] G. D. Nguyen, H.-Z. Tsai, A. A. Omrani, T. Marangoni, M. Wu, D. J. Rizzo, G. F. Rodgers, R. R. Cloke, R. A. Durr, Y. Sakai, et al., *Nat. Nanotechnol.* **2017**, *12*, 1077–1082.
- [40] M. Treier, C. A. Pignedoli, T. Laino, R. Rieger, K. Müllen, D. Passerone, R. Fasel, *Nat. Chem.* **2011**, *3*, 61–67.
- [41] P. Ruffieux, J. Cai, N. C. Plumb, L. Patthey, D. Prezzi, A. Ferretti, E. Molinari, X. Feng, K. Müllen, C. A. Pignedoli, et al., *ACS Nano* **2012**, *6*, 6930–6935.
- [42] C. Rogers, C. Chen, Z. Pedramrazi, A. A. Omrani, H.-Z. Tsai, H. S. Jung, S. Lin, M. F. Crommie, F. R. Fischer, *Angew. Chem. Int. Ed.* **2015**, *54*, 15143–15146; *Angew. Chem.* **2015**, *127*, 15358–15361.
- [43] O. Gröning, S. Wang, X. Yao, C. A. Pignedoli, G. Borin Barin, C. Daniels, A. Cupo, V. Meunier, X. Feng, A. Narita, et al., *Nature* **2018**, *560*, 209–213.
- [44] D. J. Rizzo, G. Veber, T. Cao, C. Bronner, T. Chen, F. Zhao, H. Rodriguez, S. G. Louie, M. F. Crommie, F. R. Fischer, *Nature* **2018**, *560*, 204–208.
- [45] N. Pavliček, A. Mistry, Z. Majzik, N. Moll, G. Meyer, D. J. Fox, L. Gross, *Nat. Nanotechnol.* **2017**, *12*, 308–311.
- [46] N. Pavliček, B. Schuler, S. Collazos, N. Moll, D. Pérez, E. Guitián, G. Meyer, D. Peña, L. Gross, *Nat. Chem.* **2015**, *7*, 623–628.
- [47] B. Schuler, S. Fatayer, F. Mohn, N. Moll, N. Pavliček, G. Meyer, D. Peña, L. Gross, *Nat. Chem.* **2016**, *8*, 220–224.
- [48] N. Pavliček, Z. Majzik, S. Collazos, G. Meyer, D. Pérez, E. Guitián, D. Peña, L. Gross, *ACS Nano* **2017**, *11*, 10768–10773.
- [49] S. Mishra, D. Beyer, K. Eimre, J. Liu, R. Berger, O. Gröning, C. A. Pignedoli, K. Müllen, R. Fasel, X. Feng, et al., *J. Am. Chem. Soc.* **2019**, *141*, 10621–10625.
- [50] J. Su, M. Telychko, P. Hu, G. Macam, P. Mutombo, H. Zhang, Y. Bao, F. Cheng, Z.-Q. Huang, Z. Qiu, et al., *Sci. Adv.* **2019**, *5*, eaav7717.
- [51] L. Talirz, H. Söde, J. Cai, P. Ruffieux, S. Blankenburg, R. Jaafar, R. Berger, X. Feng, K. Müllen, D. Passerone, et al., *J. Am. Chem. Soc.* **2013**, *135*, 2060–2063.
- [52] F. Mohn, B. Schuler, L. Gross, G. Meyer, *Appl. Phys. Lett.* **2013**, *102*, 073109–5.
- [53] J. Li, N. Merino-Díez, E. Carbonell-Sanromà, M. Vilas-Varela, D. G. de Oteyza, D. Peña, M. Corso, J. I. Pascual, *Sci. Adv.* **2018**, *4*, eaq0582.
- [54] P. Hapala, G. Kichin, C. Wagner, F. S. Tautz, R. Temirov, P. Jelínek, *Phys. Rev. B* **2014**, *90*, 1989–1989.
- [55] N. Pavliček, P. Gawel, D. R. Kohn, Z. Majzik, Y. Xiong, G. Meyer, H. L. Anderson, L. Gross, *Nat. Chem.* **2018**, *10*, 853–858.
- [56] S. Wang, L. Talirz, C. A. Pignedoli, X. Feng, K. M. U. Ilen, R. Fasel, P. Ruffieux, *Nat. Commun.* **2016**, *7*, 11507.
- [57] H. Oka, O. O. Brovko, M. Corbetta, V. S. Stepanyuk, D. Sander, J. Kirschner, *Rev. Mod. Phys.* **2014**, *86*, 1127–1168.
- [58] P. Willke, W. Paul, F. D. Natterer, K. Yang, Y. Bae, T. Choi, J. Fernández-Rossier, A. J. Heinrich, C. P. Lutz, *Sci. Adv.* **2018**, *4*, eaq1543.

- [59] K. Fukui, J. Inoue, T. Kubo, S. Nakazawa, T. Aoki, Y. Morita, K. Yamamoto, K. Sato, D. Shiomi, K. Nakasuji, et al., *Synth. Met.* **2001**, *121*, 1824–1825.
- [60] M. E. Sandoval-Salinas, A. Carreras, D. Casanova, *Phys. Chem. Chem. Phys.* **2019**, *21*, 9069–9076.
- [61] S. Kawai, S. Nakatsuka, T. Hatakeyama, R. Pawlak, T. Meier, J. Tracey, E. Meyer, A. S. Foster, *Sci. Adv.* **2018**, *4*, eaar7181.
- [62] S. Saito, S. Osumi, S. Yamaguchi, A. S. Foster, P. Spijker, E. Meyer, S. Kawai, *Nat. Commun.* **2015**, *6*, 8098.
- [63] W. L. Wang, S. Meng, E. Kaxiras, *Nano Lett.* **2008**, *8*, 241–245.
- [64] L. A. Agapito, N. Kioussis, E. Kaxiras, *Phys. Rev. B* **2010**, *82*, 201411.
- [65] W.-L. Ma, S.-S. Li, *Phys. Rev. B* **2012**, *86*, 045449.
- [66] A. D. Güçlü, P. Potasz, P. Hawrylak, *Phys. Rev. B* **2011**, *84*, 035425.
- [67] A. D. Güçlü, P. Potasz, O. Voznyy, M. Korkusinski, P. Hawrylak, *Phys. Rev. Lett.* **2009**, *103*, 246805.
- [68] S. Wickenburg, J. Lischner, H.-Z. Tsai, A. A. Omrani, A. Riss, C. Karrasch, A. Bradley, H. S. Jung, R. Khajeh, D. Wong, et al., *Nat. Commun.* **2016**, *7*, 13553.
- [69] J. Lu, H.-Z. Tsai, A. N. Tatan, S. Wickenburg, A. A. Omrani, D. Wong, A. Riss, E. Piatti, K. Watanabe, T. Taniguchi, et al., *Nat. Commun.* **2019**, *10*, 477.

Manuskript erhalten: 29. Oktober 2019

Akzeptierte Fassung online: 23. Dezember 2019

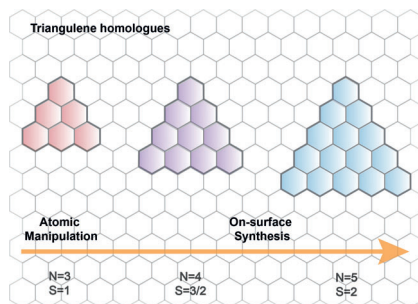
Endgültige Fassung online: ■■ ■■ ■■■■

## Kurzaufsätze

## On-Surface Synthesis

J. Su, M. Telychko, S. Song,  
J. Lu\* ————— ■■■■-■■■■

Triangulenes: from Precursor Design to  
On-Surface Synthesis and  
Characterization

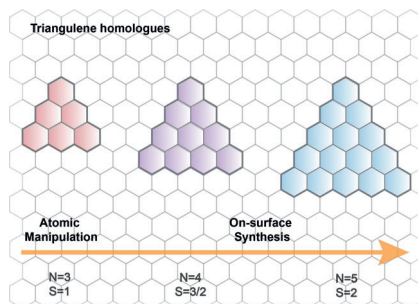


**Triangular momentum:** Synthesis and characterization of the  $[n]$ triangulene series ( $n = 3-5$ ) are presented. These open-shell molecules are predicted to host ferromagnetically coupled edge states with net spin values scaling with molecular size and are therefore considered promising candidates for future molecular spintronics applications.

## Synthese auf Oberflächen

J. Su, M. Telychko, S. Song,  
J. Lu\* ————— ■■■■-■■■■

Triangulenes: from Precursor Design to  
On-Surface Synthesis and  
Characterization



**Dreieckig, praktisch, gut:** Synthese und Charakterisierung der  $[n]$ Triangulene-Reihe ( $n = 3-5$ ) werden präsentiert. Diese offenschaligen Moleküle besitzen wahrscheinlich ferromagnetisch gekoppelte Kantenzustände mit Netto-Spinwerten, die mit der Molekülgröße skalieren. Das macht sie zu vielversprechenden Kandidaten für zukünftige Anwendungen in der molekularen Spintronik.

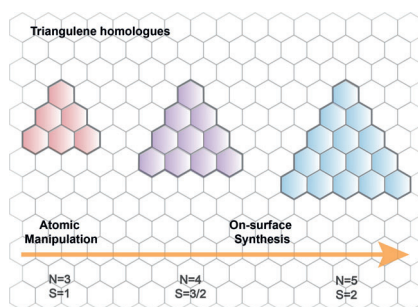
## Kurzaufsätze

## Synthese auf Oberflächen

J. Su, M. Telychko, S. Song,

J. Lu\* ————— ■■■■-■■■■

Triangulenes: from Precursor Design to  
On-Surface Synthesis and  
Characterization



**Dreieckig, praktisch, gut:** Synthese und Charakterisierung der  $[n]$ Triangulen-Reihe ( $n = 3-5$ ) werden präsentiert. Diese offenschaligen Moleküle besitzen wahrscheinlich ferromagnetisch gekoppelte Kantenzustände mit Netto-Spinwerten, die mit der Molekülgröße skalieren. Das macht sie zu vielversprechenden Kandidaten für zukünftige Anwendungen in der molekularen Spintronik.